

Electronic Supplementary Information

for

Light-Controlled Reversible Formation and Dissociation of Nanorods via Interconversion of Pseudorotaxanes

Jun Wang,^a Heng-Yi Zhang,^{*a} Xu-Jie Zhang,^a Zhi-Hui Song,^a Xiao-Jun Zhao^{*b} and
Yu Liu^{*a}

^a Department of Chemistry, State Key Laboratory of Elemento-Organic Chemistry,
Nankai University, Collaborative Innovation Center of Chemical Science and
Engineering, Tianjin 300071, P. R. China. Email: hyzhang@nankai.edu.cn,
yuliu@nankai.edu.cn

^bTianjin Normal University, Collaborative Innovation Center of Chemical Science
and Engineering, Tianjin 300072, P. R. China. Email: hsxyzxj@mail.tjnu.edu.cn

Contents

Experimental section	S3
Fig. S1-S3. Characterization of DNDS.....	S6
Fig. S4. ^1H ROESY of 2 \subset 1	S6
Fig. S5. Job's plot of 1 with 2	S7
Fig. S6. ESI-MS spectrum of 2 \subset 1	S7
Fig. S7. absorption spectra and optical transmittance of 1	S8
Fig. S8. absorption spectra and optical transmittance of 2	S8
Fig. S9. Detection of host 1 -induced CAC of guest 2	S9
Fig. S10. Optical transmittance of 2 with 1 and building block.....	S9
Fig. S11. Zeta Potential of nanorods.....	S10
Fig. S12. ^1H ROESY of 2 \subset 1 $\cdot\alpha$ -CD.....	S11
Fig. S13. ESI-MS spectrum of 2 \subset 1 $\cdot\alpha$ -CD.....	S11
Fig. S14. TEM image of 2 \subset 1 $\cdot\alpha$ -CD.....	S12
Fig. S15. Absorption spectra of 3 $\subset\alpha$ -CD.....	S12
Fig. S16. Circular dichroism change of 3 $\subset\alpha$ -CD upon Vis/UV irradiation.....	S13
Fig. S17. Circular dichroism spectra of different mixture solution.....	S13
Fig. S18. Controlling TEM images.....	S14
Fig. S19. Absorption spectra of 3 with 2 \subset 1 $\cdot\alpha$ -CD upon Vis/UV irradiation.....	S14
Fig. S20. Circular dichroism change of 3 with 2 \subset 1 $\cdot\alpha$ -CD upon Vis/UV irradiation.	S15

Experimental Section

General Method. All chemicals were commercially available and were used without further purification unless noted otherwise. Compounds **1**, **2** and **3** were synthesized according to the previous reports.^{1,2,3} The synthesis of 4,8-dimethoxy-naphthalene-1,5-disulfonate sodium (DNDS) was described in the following, and it was identified by NMR spectroscopy in D₂O, performed on a Varian 400 spectrometer, mass spectrometry, performed on an IonSpec QFT-ESI MS, which were listed in Figures **S1–S3**, respectively. RPMI-1640 culture solution purchased Gibco company and the HGC-27 gastric cells were provided by Beijing tumor biology test center.

Preparation of stocks solution

A predetermined amount of **1**, **2**, **3** and α -CD were dissolved in aqueous phosphate-buffered saline (PBS) buffer to gain 1 mM stock solutions. Corresponding bulk of the above stock solutions were mixed for each measurement.

UV-Vis Spectra and Optical Transmittance

UV-Vis spectra and optical transmittance were recorded in a quartz cell (light path 10 mm) on a Shimadzu UV-3600 spectrophotometer equipped with a PTC-348WI temperature controller.

TEM and SEM Experiments

TEM images were recorded on a Philips Tecnai G2 20S-TWIN microscope operating at an accelerating voltage of 200 keV. The sample for TEM measurements was prepared by dropping the solution onto a copper grid. The grid was then air-dried. SEM images were recorded on a Hitachi S-3500N scanning electron microscope. The

sample for SEM measurements was prepared by dropping the solution onto a coverslip, followed by evaporating the liquid in air.

Zeta Potential measurements

Zeta Potential experiment was carried out on a Zetasizer Nano ZS from Brookhaven Instruments equipped with a 10 mW HeNe laser at a wavelength of 633 nm.

Synthesis of 4,8-dimethoxy-naphthalene-1,5-disulfonate sodium (DNDS). We have synthesized host **1** building subunit according our previous article.^{S1} The process of synthesis was as follows: 2.33 g (20.00 mmol) chlorosulfonic acid was added dropwise over a period of 2 h to a stirred solution of 1,5-dimethoxynaphthalene (0.38 g, 2 mmol) in dry 150 mL CHCl₃ at -5 °C. After additional 4 h reaction at -5 °C, a white precipitate was obtained. The precipitate was carefully collected by filtration and washed with 50 mL dry CHCl₃ at once. The residue was taken up into 100 mL H₂O, and 5% NaOH solution was added until pH = 7. The solvate was envapoured and the residue was recrystallized from acetonitrile-acetone for three times and dried by vacuum, the target compound was obtained as white solid (731 mg, 91%).

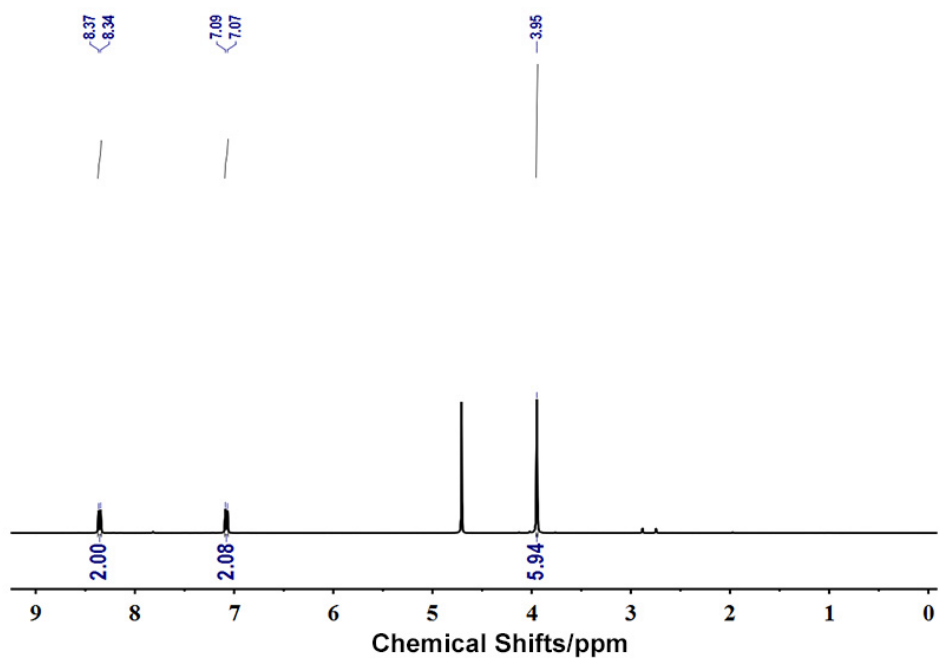


Fig. S1. ^1H NMR spectrum (400 MHz, D_2O , 25 $^\circ\text{C}$) of DNDS.

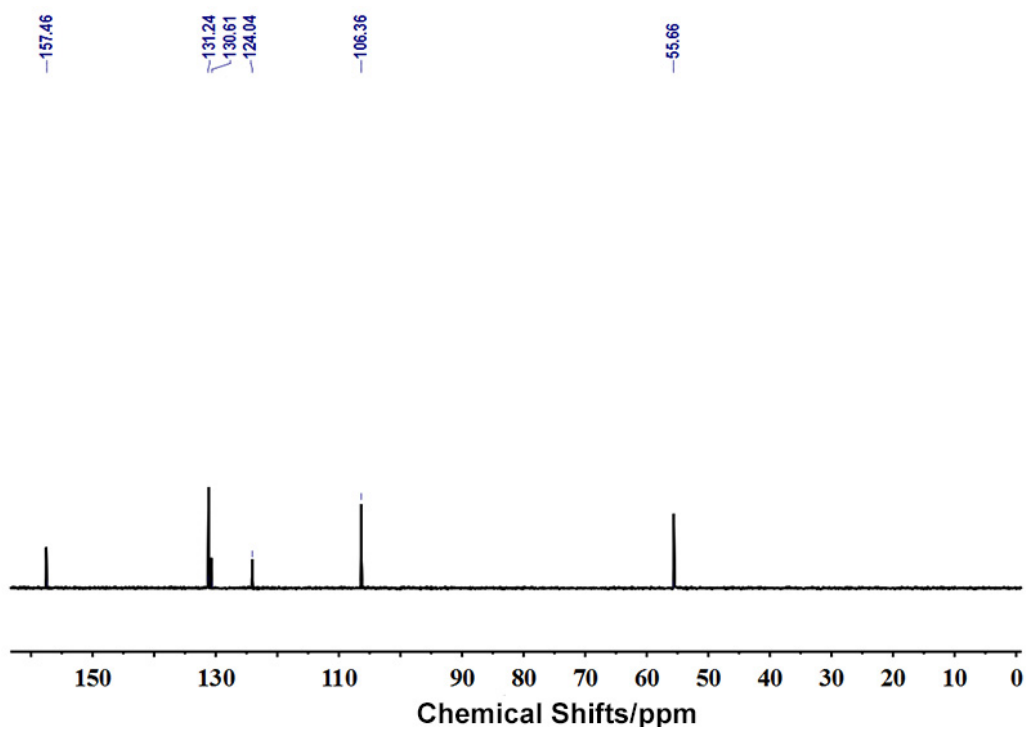


Fig. S2. ^{13}C NMR spectrum (100 MHz, D_2O , 25 $^\circ\text{C}$) of DNDS.

Sample Name	lc/ms	Position	P1-A3	Instrument Name	Instrument 1	User Name	
j Vol	2	InjPosition	chen-ms.m	SampleType	Sample	IRM Calibration Status	Some Ions Missed
sta Filename	WJ-416.d	ACQ Method	chen-ms.m	Comment		Acquired Time	7/26/2013 4:12:09 F

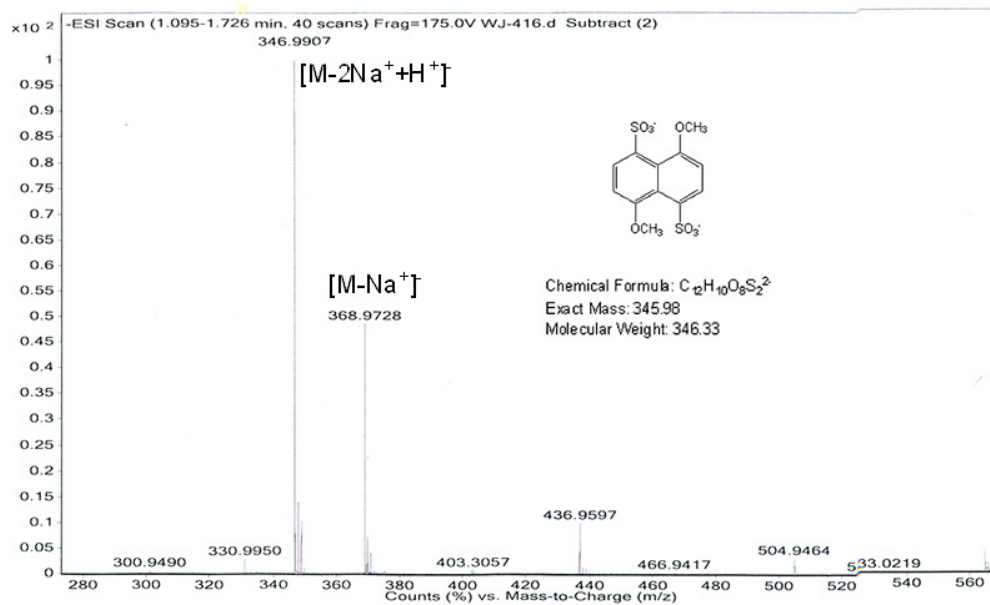


Fig. S3. ESI-HRMS spectrum of DNDS.

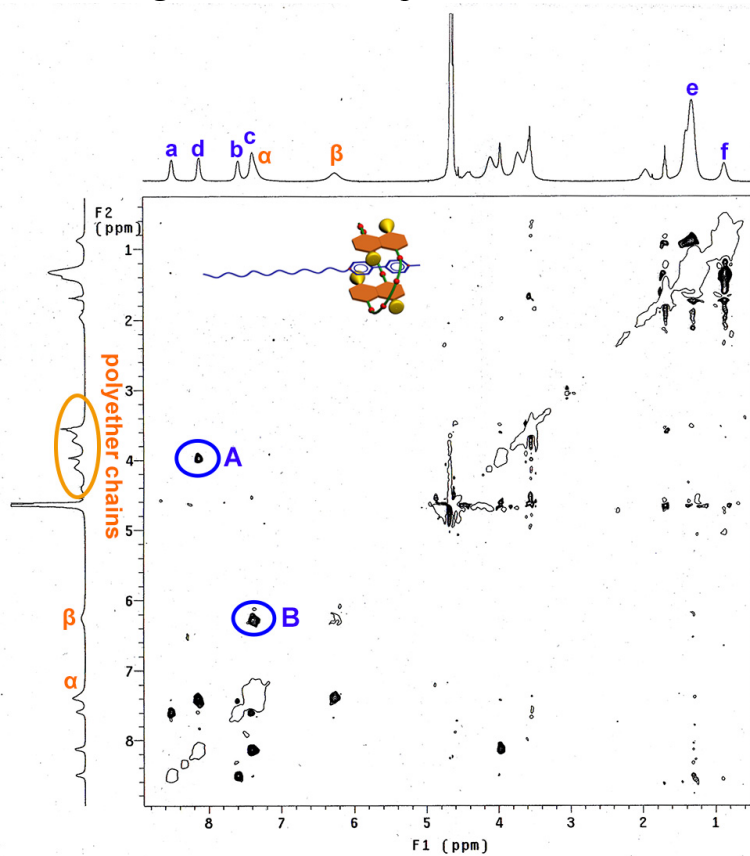


Fig. S4. 1H ROESY spectrum of [2]pseudorotaxane **2c1** in D_2O at $25\text{ }^\circ C$.

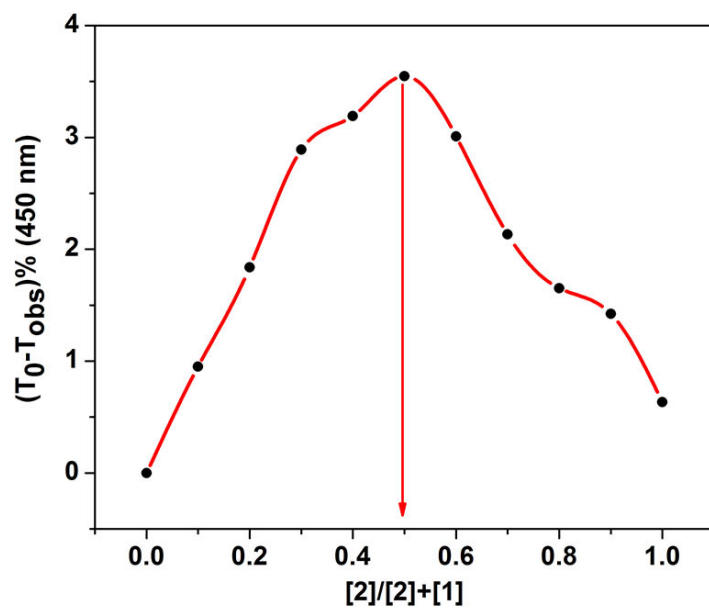


Fig. S5. Job's plot of [2]pseudorotaxane **2c1** at total concentration of 0.01 mM at 25 °C.

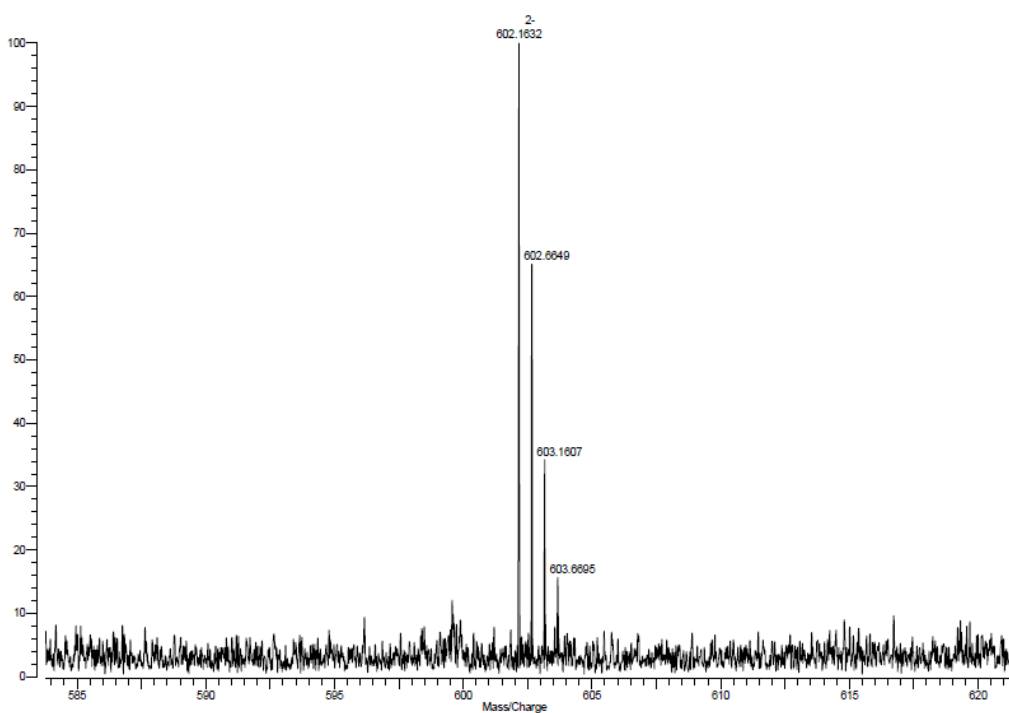


Fig. S6. ESI-MS spectrum of [2]pseudorotaxane **2c1**. The peak at m/z 602.1632 is assigned to $[1 + 2]^{2-}$, calcd.: 602.1624.

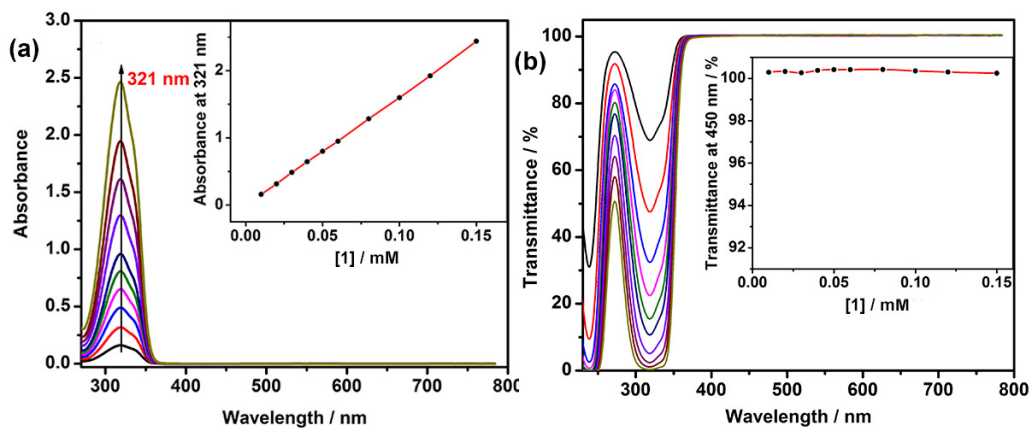


Fig. S7. UV-Vis absorption spectra (a) and optical transmittance (b) of host **1** at different concentrations (from 0.01 mM to 0.15 mM) at 25 °C in water. Inset: dependence of (a) the absorbance at 321 nm and (b) optical transmittance at 450 nm on **1** concentration, respectively.

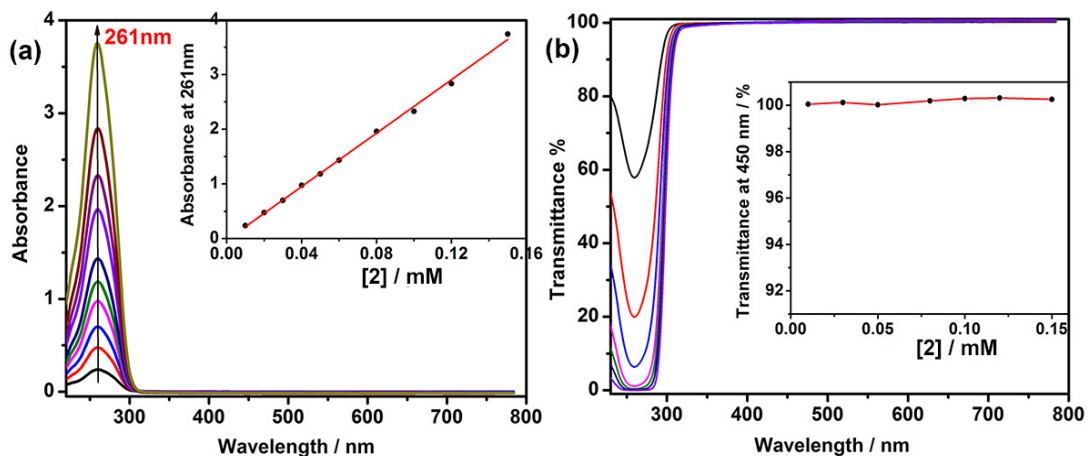


Fig. S8. UV-Vis absorption spectra (a) and optical transmittance (b) of guest **2** at different concentrations from 0.01 mM to 0.15 mM at 25 °C. Inset: dependence of the absorption at 261 nm (a) and optical transmittance at 450 nm on **2** concentration, respectively.

It should be noted that there was no obvious changes at longer wavelength region, and good linear relationship between absorbance or optical transmittance and the $1/2$ concentration from 0.01 to 0.15 mM, indicating that free $1/2$ was without any self-

aggregation behaviors under the concentration conditions.

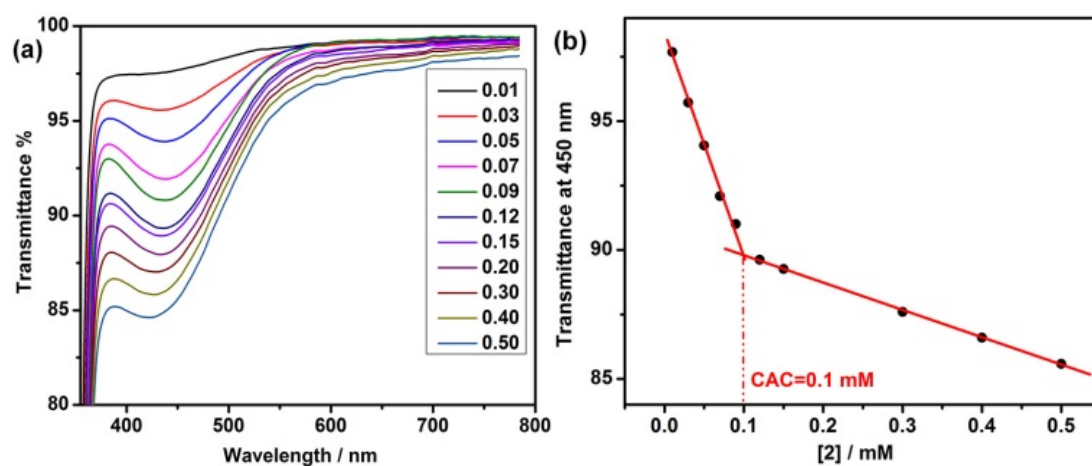


Fig. S9. (a) Dependence of the optical transmittance at 25 °C on **2** concentration in the presence of 0.1 mM **1**; (b) The corresponding CAC was determined to be 0.1 mM.

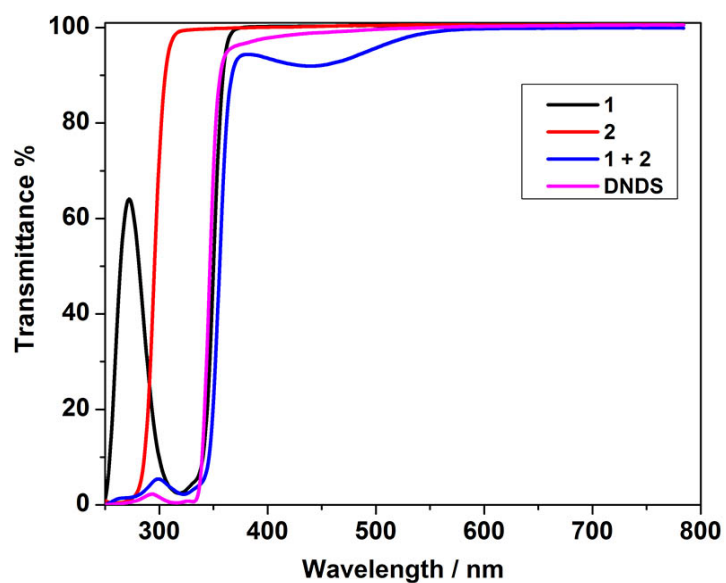
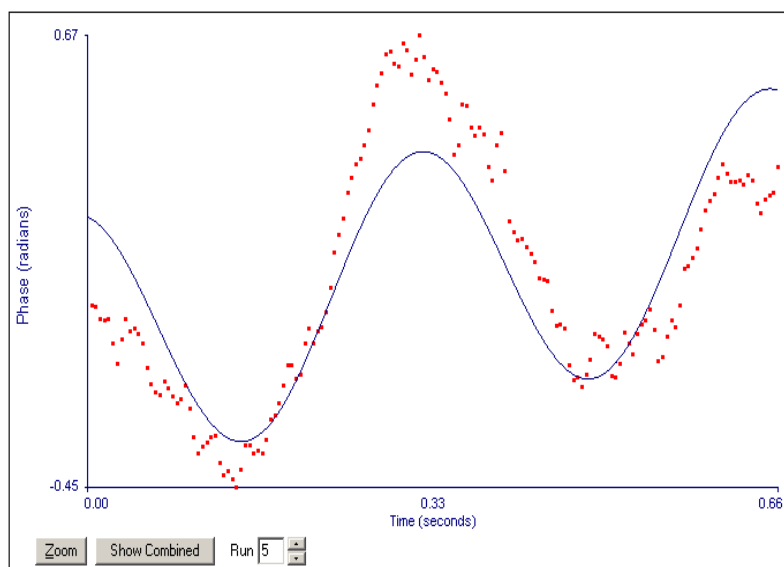


Fig. S10. Optical transmittance of **1**, **2**, **1 + 2** and **2 + DNDS** at 25 °C in water; [**1**] = 0.1 mM, [**2**] = 0.1 mM, [DNDS] = 0.20 mM, respectively.



Run	Mobility	Zeta Potential (mV)	Rel. Residual	Measurement Parameters:
1	-0.73	-9.33	0.0087	Conductance = 133 μ S
2	-0.76	-9.75	0.0141	Current = 0.28 mA
3	-0.66	-8.42	0.0077	Electric Field = 5.24 V/cm
4	-0.75	-9.56	0.0065	Sample Count Rate = 965 kcps
5	-0.55	-7.00	0.0122	Ref. Count Rate = 1933 kcps
				Uncorrected Temp. = 25.5 °C
Mean	-0.69	-8.81	0.0098	
Std. Error	0.04	0.51	0.0014	
Combined	-0.68	-8.69	0.0057	

Fig. S11. Zeta Potential of [2]pseudorotaxane 2C1 nanorods, [1] = [2] = 0.1 mM.

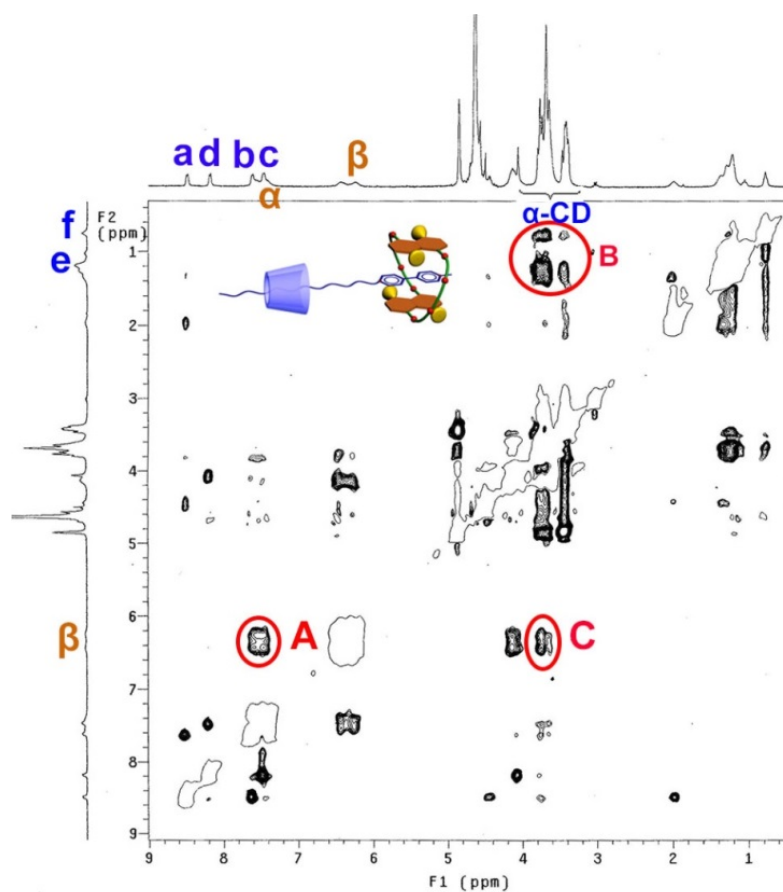


Fig. S12. ^1H ROESY spectrum of $[3]\text{pseudorotaxane } 2\text{C}1 \cdot \alpha\text{-CD}$ in D_2O at $25\text{ }^\circ\text{C}$.

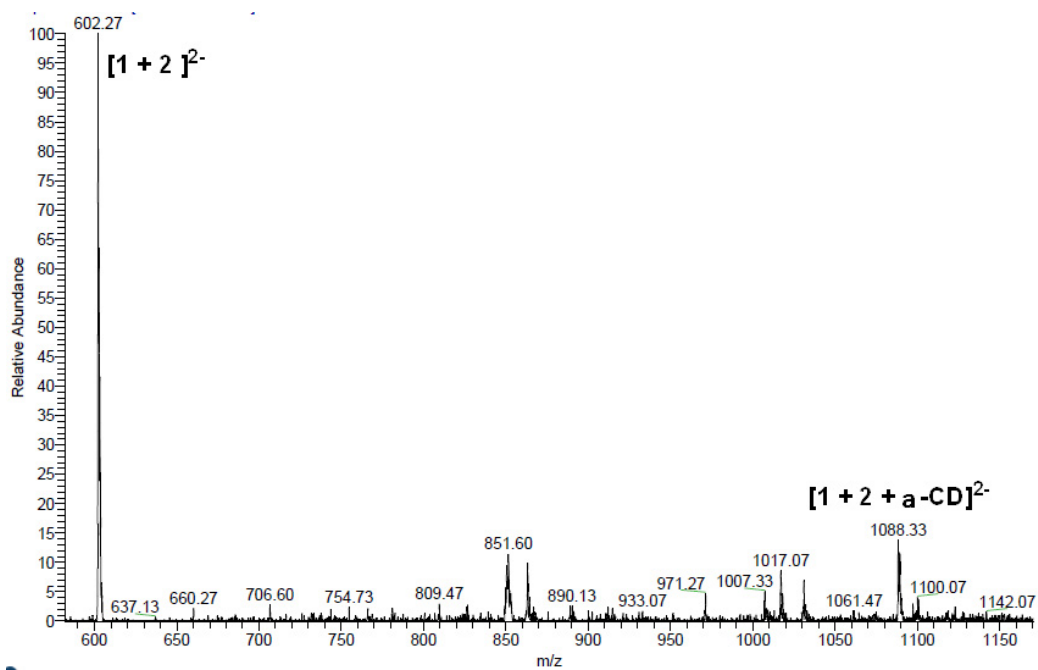


Fig. S13. ESI-MS spectrum of $[3]\text{pseudorotaxane } 2\text{C}1 \cdot \alpha\text{-CD}$. The peak at m/z 602.27 is assigned to $[1 + 2]^{2-}$, calcd.: 602.16; the peak at m/z 1088.33 is assigned to $[1 + 2 + \alpha\text{-CD}]^{2-}$, calcd.: 1088.32.

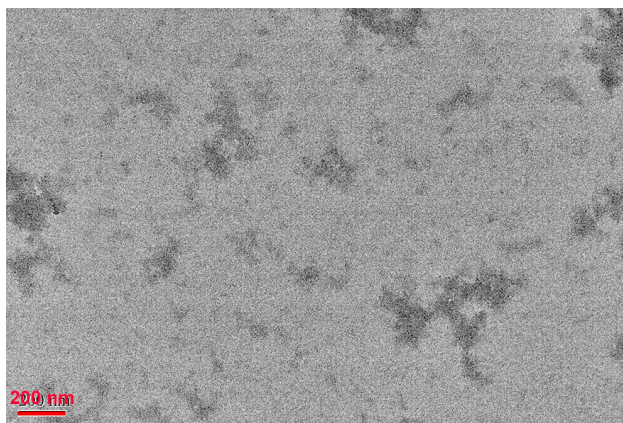


Fig. S14. TEM image of [2]pseudorotaxane **2C1** aggregates in the presence of excess α -CD, $[1] = [2] = 0.1$ mM, $[\alpha\text{-CD}] = 0.5$ mM.

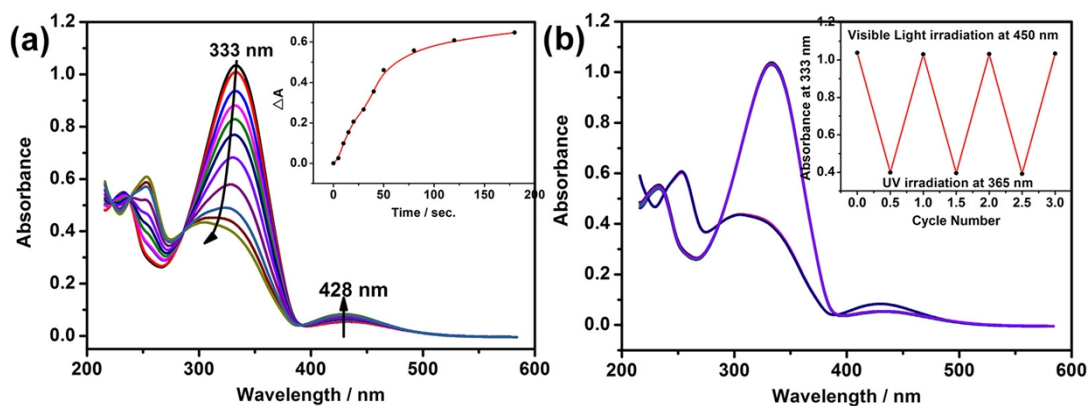


Fig. S15. (a) Absorption spectra of **3C** α -CD in water after UV irradiation at 365 nm, Inset: Absorbance changes at 333 nm versus irradiation time. (b) Cycling of the photo-mediated *trans* and *cis* isomerization of **3C** α -CD ($[3] = [\alpha\text{-CD}] = 0.05$ mM) by alternate irradiation with UV and visible light at 25 °C.

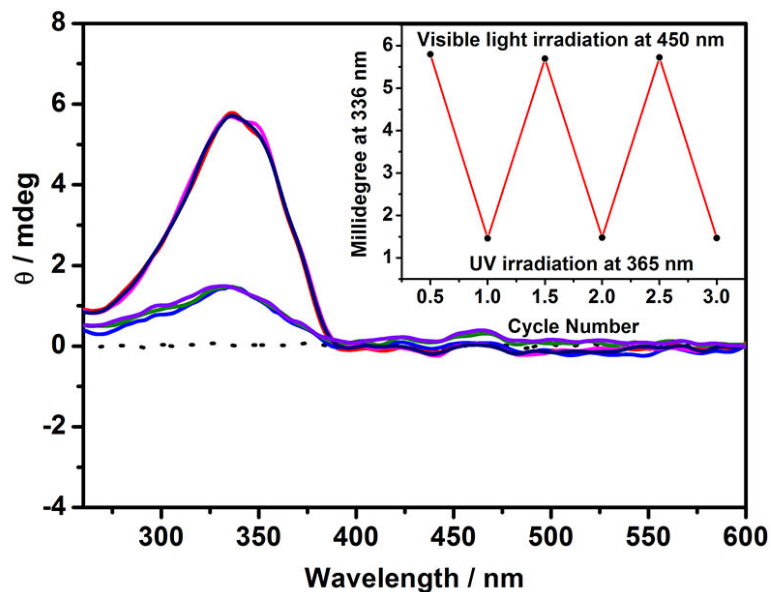


Fig. S16. Circular dichroism changes of mixture solution of **3** + α -CD upon alternate irradiation with UV and visible light. Inset: Cycling of the photo-mediated *trans* and *cis* isomerization of **3** in the mixture ($[3] = [\alpha\text{-CD}] = 0.1 \text{ mM}$, $25 \text{ }^\circ\text{C}$, respectively).

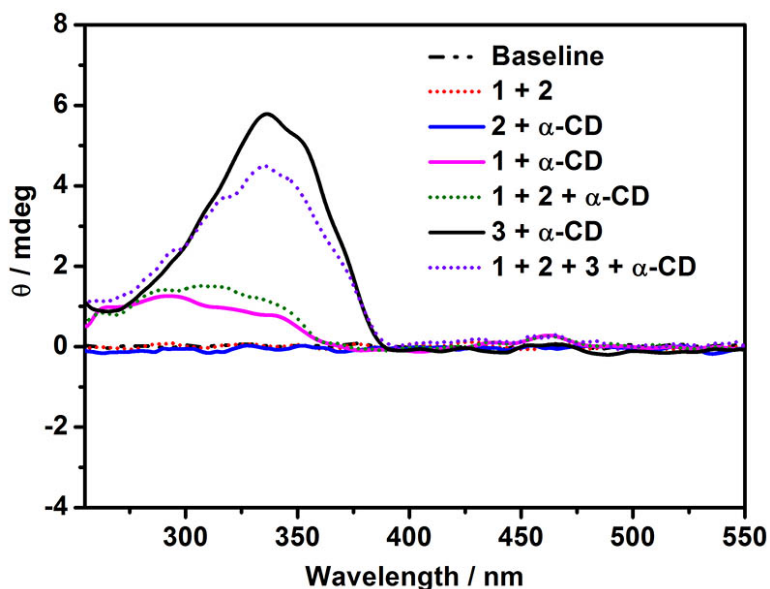


Fig. S17. Circular dichroism spectra of different components of **1** + **2**, **2** + α -CD, **1** + α -CD, **1** + **2** + α -CD, **3** + α -CD and four-components mixture of **1** + **2** + α -CD + **3**, ($[1] = [2] = [\alpha\text{-CD}] = 0.1 \text{ mM}$, $[3] = 0.5 \text{ mM}$, $25 \text{ }^\circ\text{C}$, respectively).

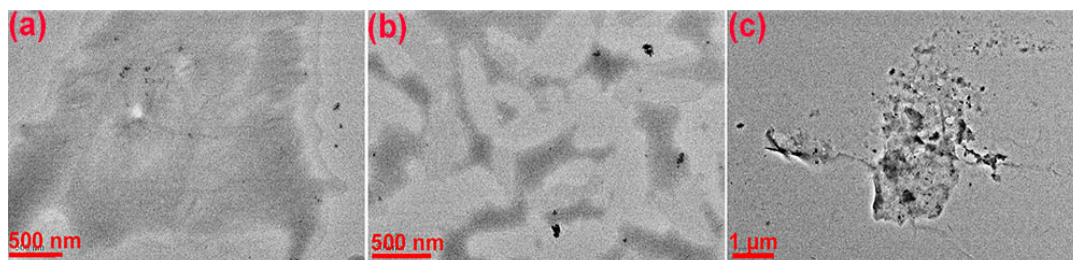


Fig. S18. TEM images of (a) α -CD + **3**, (b) **1** + α -CD + **3**, (c) **1** + α -CD. [**1**] = 0.1 mM, [α -CD] = 0.2 mM, [**3**] = 0.3 mM, respectively).

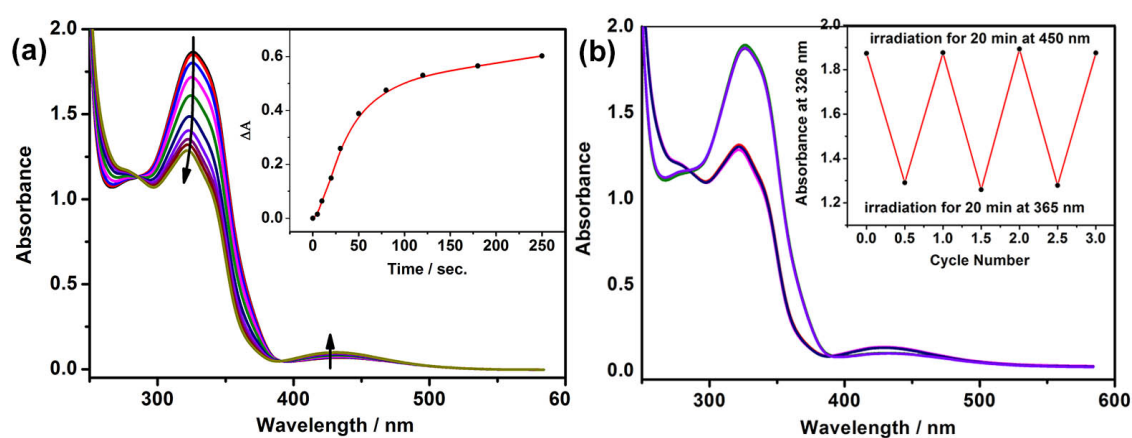


Fig. S19. (a) Absorption spectra of a four-components mixture of [**3**]pseudorotaxane $2\subset 1\cdot\alpha$ -CD + **3** after UV irradiation at 365 nm, Inset: Absorbance changes at 326 nm versus irradiation time. (b) Cycling of the photo-mediated *trans* and *cis* isomerization of the quaternary mixture ([**1**] = [α -CD] = 0.05 mM) by alternate irradiation with UV and visible light at 25 °C, ([**1**] = [**2**] = [α -CD] = [**3**] = 0.05 mM, respectively).

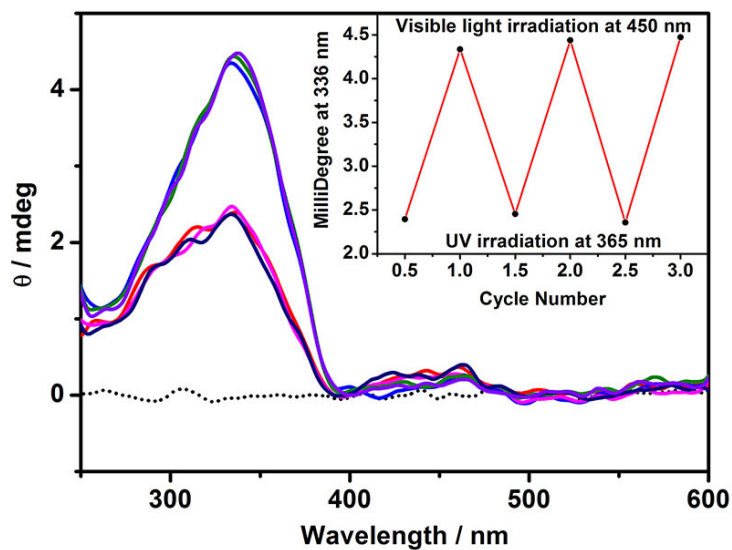


Fig. S20. Circular dichroism changes of the four-components mixture of [3]pseudorotaxane **2**⊂**1**· α -CD + **3** upon alternate irradiation with UV and visible light. Inset: Cycling of the photo-mediated *trans* and *cis* isomerization of **3** in the quaternary mixture ($[\mathbf{1}] = [\mathbf{2}] = [\alpha\text{-CD}] = 0.1 \text{ mM}$, $[\mathbf{3}] = 0.5 \text{ mM}$, $25 \text{ }^\circ\text{C}$, respectively).

Generally, azobenzene isomerizes to predominantly *trans* and *cis* forms under visible (Vis) and ultraviolet (UV) light, respectively.⁴ According to previous reports,⁵ we can conclude that the photoisomerization of azophenyl unit is a crucial factor to govern the formation and dissociation of inclusion complex between azobenzene and α -CD. The ^1H NMR of **1** + **2** + **3** + α -CD after UV irradiation in Fig. 3f (in the text), the Fig. S17, Fig. S19 & S20 jointly indicate the reversibility of the azobenzene photoisomerization in four-components solution, along with the transfer of α -CD from **3**⊂ α -CD to amphiphilic [2]pseudorotaxane **2**⊂**1**. As a result, owing to the formation and dissociation of inclusion complex **3**⊂ α -CD, a reversible conformational change in the transition from amphiphilic [2]pseudorotaxane **2**⊂**1** to water-soluble

[3]pseudorotaxane 2 \subset 1 \cdot α -CD can be operated by the azobenzene photoisomerization. Combining these spectroscopic, NMR (Fig. 3f) of four-components system after UV irradiation and microscopic investigation results, we can speculate the reversibility of the assembly and disassembly processes was driven by the azobenzene photoisomerization in four-components solution.

References:

-
- [1] L. Chen, H. Zhang and Y. Liu, *J. Org. Chem.*, 2012, **77**, 9766.
[2] Y. Lei, *J. Phys. Chem.*, 1991, **95**, 7918.
[3] D. Liu, Y. Xie, H. Shao and X. Jiang, *Angew. Chem. Int. Ed.* 2009, **48**, 4406.
[4] H. M. D. Bandarab and S. C. Burdette, *Chem. Soc. Rev.*, 2012, **41**, 1809.
[5] (a) X. Liao, G. Chen, X. Liu, W. Chen, F. Chen and M. Jiang, *Angew. Chem. Int. Ed.*, 2010, **49**, 4409. (b) X. Ma, Q. Wang, D. Qu, Y. Xu, F. Ji and H. Tian, *Adv. Funct. Mater.* 2007, **17**, 829. (c) S. K. M. Nalluri and B. J. Ravoo, *Angew. Chem. Int. Ed.*, 2010, **49**, 5371. (d) I. Tomatsu, A. Hashidzume and Akira Harada, *J. Am. Chem. Soc.*, 2006, **128**, 2226.